ChemComm

COMMUNICATION

View Article Online
View Journal | View Issue

Cite this: *Chem. Commun.*, 2018, **54**, 13115

Received 12th September 2018,
Accepted 29th October 2018

DOI: 10.1039/c8cc07410k

rsc.li/chemcomm

A fluoride activated methylene blue releasing platform for imaging and antimicrobial photodynamic therapy of human dental plaque†

Peng Wei,[a] Fengfeng Xue,[a] Yunming Shi,[b] Ross Strand,[b] Hui Chen [a] and Tao Yi *[a]

We report a F^- activated methylene blue (MB) releasing platform for imaging and antimicrobial photodynamic therapy (aPDT). By utilizing this platform, one of the selected probes, FD-F3, displays a remarkable near-infrared fluorescence and absorption increase towards F^- with good selectivity and low detection limit. This probe has been successfully applied for visualizing F^- and performing F^- activated aPDT in naturally grown human plaque biofilms.

Fluoride, the smallest anion, occurs naturally in many water sources and is widely used as an anti-caries agent.[1,2] Fluoride can be absorbed by the dental plaque biofilm as a fluoride reservoir in the oral cavity. When demineralization occurs, fluoride anions can be released from the reservoir to promote remineralization in combination with calcium and phosphate ions.[3,4] Adequate uptake of fluoride is necessary for the prevention of tooth decay, for enhancing the remineralization of enamel and for inhibiting the demineralization of enamel and root surfaces.[5,6] However, over-exposure to fluoride may cause issues such as skeletal fluorosis and kidney problems.[1,7,8] Therefore, it is of vital importance to develop accurate tools that can be used to monitor fluoride, especially those that can work in human dental plaque biofilms.

To help determine F^- quickly and easily, fluorescent chemical sensors are of interest because of their high sensitivity, speed of detection and ease of operation.[9,10] The greatest advantage of a fluorescent sensor is that it can be used *in situ* to detect F^- in a biosystem *via* fluorescence imaging. Until now, many fluorescent probes have been designed to exploit the unique reactivity of F^-, using different mechanisms, including F^- induced cleavage reactions,[11–18] nucleophilic addition reactions[19] and supramolecular interactions (including our previous works).[20–24] In all these mechanisms, a desilylation reaction based strategy, developed by Kim and Swager in 2003, has a high selectivity toward F^- compared with other design strategies due to the high affinity of fluoride for silicon,[25] which is propitious to our goal of developing a novel platform for the detection and visualization of F^- in a bio system (naturally grown human plaque biofilms).

On the other hand, bacteria living in the dental plaque biofilm can lead to periodontal diseases (gingivitis or periodontitis). Mechanical removal of dental plaque is currently the most frequently used method to treat periodontal diseases. Although different kinds of antimicrobial agents have been used, the desired effect has not been achieved because bacteria growing in biofilms always exhibit resistance to antimicrobial agents.[26] Therefore, antimicrobial photodynamic therapy (aPDT), in which the energy of light can be transformed to $^3O_2$ to generate singlet oxygen by irradiating a photosensitizer (PS) with light at certain wavelengths, has emerged as one of the most efficient treatment alternatives to chemical antimicrobial agents.[26–28] aPDT can efficiently kill the bacteria exposed to the light with the help of PS and avoid producing drug resistance. Just recently, we reported a deformylation reaction-based fluorescent probe for *in vivo* imaging of HOCl using methylene blue (MB) as the fluorophore.[29] Given that MB is one of the most widely used agents for aPDT and fluoride is enriched in plaque bacteria, a new idea comes to us that we can design a MB based platform for sensing F^-. The platform can selectively respond to F^- to release MB which acts both as a near-infrared fluorescent probe for imaging F^- and an effective PS for aPDT in the dental plaque biofilm.

A desilylation reaction based strategy was used for this objective. Although numerous organosilicon compounds have been reported to detect F^- based on different fluorophore platforms including boron-dipyrromethenes (BODIPYs),[11] coumarins,[12,13] cyanines,[14,15] fluoresceins,[30,31] naphthalimides[16] and thiazoles,[17,18] none of these probes have been used for imaging F^- in dental plaque biofilms nor have they been applied as F^- regulated antimicrobial reagents. In this work, we developed a new F^- activated MB fluorophore releasing platform (**FD-F*n***) for F^- sensing and aPDT in a dental plaque biofilm for the first time.

[a] *Department of Chemistry, Fudan University, 2005 Songhu Road, Shanghai 200438, China. E-mail: yitao@fudan.edu.cn*
[b] *P&G Technology (Beijing) Co., Ltd., No. 35 Yuan Road, B zone, Shunyi District, Beijing, 101312, China*

† Electronic supplementary information (ESI) available: Experimental details, additional tables, spectra and images. See DOI: 10.1039/c8cc07410k

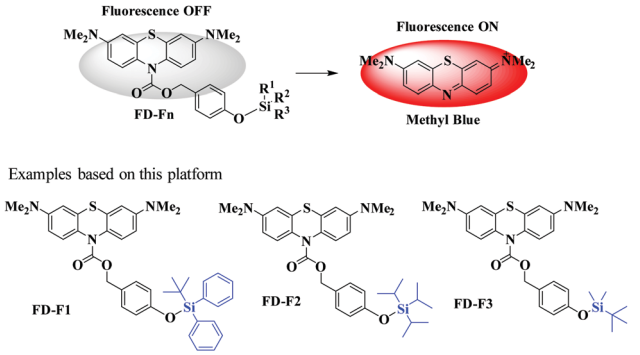

Scheme 1 The fluoride activated MB releasing platform and three candidate compounds in this work.

Three fluorescent probes **FD-F1**, **FD-F2** and **FD-F3** were designed and synthesized by linking leucomethylene blue (the reduced form of MB) with *tert*-butyldiphenylsilyl (TBDPS), triisopropylsilyl (TIPS) and *tert*-butyldimethylsilyl (TBDMS), respectively, as the reaction group (Scheme 1) to prove the feasibility of this platform. The detection capability of the three candidate compounds towards F^- was evaluated by the comparison of the spectral changes of these compounds with the addition of F^-. In the absence of NaF, all three compounds showed no absorption or fluorescence emission in the visible and longer wavelength range because of the small conjugation system of the compounds (Fig. 1a, b and Fig. S1, S2, ESI†), and could maintain stability even after 24 h of incubation under physiological conditions (Fig. S3, ESI†). All of these compounds could react with NaF, as shown in Fig. 1a and b and Fig. S1, S2 (ESI†), with the absorption, emission, extinction coefficient, fluorescent quantum yields and brightness drastically enhanced (Table S1, ESI†) due to a F^- triggered cleavage of the Si–O bond to afford the common dye MB (Scheme 1). The reaction mechanism was further confirmed by HRMS and HPLC analyses in aqueous solution, as shown in Fig. S5–S8 (ESI†). However, among the three compounds, **FD-F3** shows much greater changes in fluorescence intensity (at 690 nm) and absorbance (at 667 nm) than those of **FD-F1** and **FD-F2** after reaction with NaF (Fig. 1a, b and Fig. S1, S2, ESI†). For example, after treatment with 50 equiv. of F^- for 50 min, the fluorescence intensity of **FD-F3** at 690 nm increased 996-fold and the absorbance at 667 nm increased 499-fold with the formation of the MB fluorophore, much larger than that of **FD-F1** and **FD-F2** under the same conditions (**FD-F1**, FL intensity: 10-fold, Abs: 8-fold, Fig. S1, ESI;† **FD-F2**, FL intensity: 24-fold, Abs: 20-fold, Fig. S2, ESI†). Meanwhile, the quantitative analysis by HPLC showed that the MB release efficiencies of the three probes were **FD-F3** (96.9%) > **FD-F2** (45.9%) > **FD-F1** (36.9%) (Table S2, ESI†), which were consistent with the results of the spectral test. This may be due to the larger steric hindrance around the silicon atom of **FD-F1** or **FD-F2** than that of **FD-F3**, which hinders the fluoride ion attack on silicon. These data indicated that all three of the candidate compounds could be used to detect NaF and **FD-F3** was the optimal compound with regard to its sensitivity towards NaF.

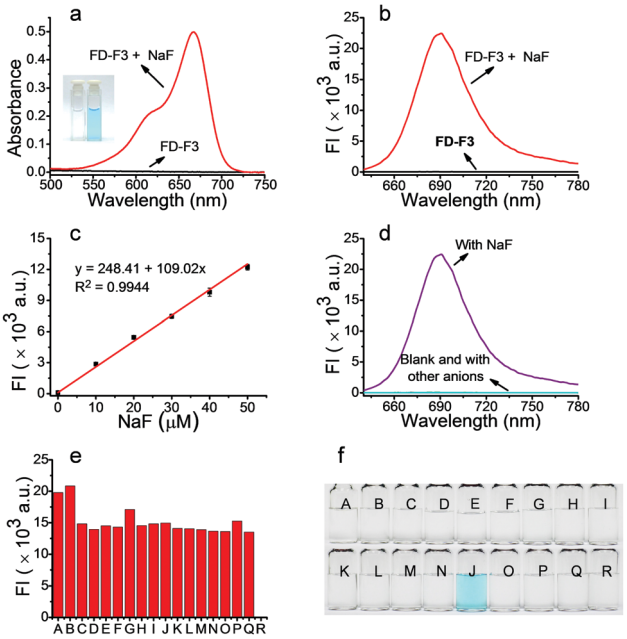

Fig. 1 (a) Absorption and (b) fluorescence spectra of **FD-F3** (10 μM) before and after treatment with 500 μM NaF for 50 min. Inset in a is the picture before (left) and after (right) treatment with NaF; (c) linear relationship between fluorescence intensity at 690 nm and concentrations of NaF; (d) fluorescence intensity at 690 nm with 500 μM of various analytes and (e) with 500 μM of various analytes in the presence of 500 μM NaF (A: CO_3^{2-}, B: PO_4^{3-}, C: $H_2PO_4^-$, D: NO_3^-, E: NO_2^-, F: SO_4^{2-}, G: SO_3^{2-}, H: $S_2O_3^{2-}$, I: CH_3COO^-, J: F^-, K: Cl^-, L: Br^-, M: I^-, N: N_3^-, O: SCN^-, P: $C_2O4_2^-$, Q: BSA, and R: blank); (f) colour change of **FD-F3** (10 μM) after treatment with 500 μM of various analytes. Conditions: incubated for 50 min, DMSO-HEPES solution (3/2, v/v, 10 mM HEPES, pH = 7.2), and λ_{ex} = 620 nm.

High-level selectively is of paramount importance for an effective chemosensor. With the promising sensitivity to F^-, we then explored the selectivity of **FD-F3** with different anions. As shown in Fig. 1d and Fig. S9 (ESI†), **FD-F3** showed no fluorescence intensity and absorbance changes upon treatment with 500 μM of various anions including CO_3^{2-}, PO_4^{3-}, $H_2PO_4^-$, NO_3^-, NO_2^-, SO_4^{2-}, SO_3^{2-}, $S_2O_3^{2-}$, CH_3COO^-, Cl^-, Br^-, I^-, N_3^-, SCN^-, $C_2O_4^{2-}$, and BSA. Competitive studies were also carried out to study any interference of the above mentioned anions on F^- detection (Fig. 1e). The result showed that the addition of other anions had no negative impact on **FD-F3** for sensing F^-, revealing the extremely high selectivity of **FD-F3** for F^- and that only F^- resulted in the dramatic increase in both fluorescence intensity and absorbance with an obvious colour change. All the other anions showed almost no changes in fluorescence or absorbance (Fig. 1f).

To determine the practical pH range of **FD-F3** as the F^- probe, the fluorescence changes of **FD-F3** at 690 nm before/after treatment with NaF at different pH levels were assessed (Fig. S10, ESI†). Studies show that **FD-F3** could remain stable in a pH range of 2–12. When treated with NaF, a dramatic fluorescence intensity enhancement was observed over the pH range of 5–12, indicating that **FD-F3** could be used in conventional environments.

Several different fluoride sources are used as additives to fulfil different requirements. For example, sodium fluoride

(NaF) and sodium monofluorophosphate (SMFP) are the most common fluoride additives used in commercial dental hygiene products.[32] So, we measured whether **FD-F3** could be activated by F^- from different sources. As shown in Fig. S11 (ESI†) both organic fluorides and inorganic fluorides could cause drastic fluorescence intensity changes in **FD-F3**. In addition, concentration-dependent studies found that **FD-F3** could quantitatively detect F^- from different sources. The fluorescence intensity of **FD-F3** at 690 nm showed a good linear relationship with the concentration of NaF in the range of 0–50 μM (Fig. 1c) and SMFP in the range of 0–1000 μM (Fig. S12, ESI†). The detection limit was calculated to be 0.16 μM for NaF and 1.23 μM for SMFP. These data illustrated that **FD-F3** could not only detect F^- but also identify F^- from different sources.

Since **FD-F3** performed well in the aforementioned tests in an aqueous solution, we further explored the application of **FD-F3** to determine the F^- content of toothpastes prepared from different fluoride sources and in dental plaque biofilms. The F^- content in water with different fluoride sources was measured using a standard addition method to evaluate the accuracy of the detection method. The result showed that F^- from different sources could be accurately measured with good recovery (from 90.3% to 105.7%) (Table S3, ESI†), indicating that **FD-F3** could quantitatively detect F^- precisely in water samples and be further used in real samples.

Table 1 shows the measured concentrations of different fluoride sources in toothpastes using the proposed method based on **FD-F3**, compared with the calculated value based on the annotated content on the toothpaste packaging. For comparison, the fluoride concentration was also measured by FISE which is a type of ion selective electrode that is sensitive to the concentration of F^-. As shown in Table 1, when a toothpaste using NaF as the F^- source was tested, the measured NaF content using **FD-F3** was closer to the annotated content than that from FISE. This indicates that for the selected sample the fluorescence method using **FD-F3** as a detector for quantitative fluoride analysis was more accurate than the FISE method. Meanwhile, for the toothpaste using SMFP as the F^- source, the measured SMFP contents using **FD-F3** and the traditional FISE method were both far lower than the annotated content, which implied that the real SMFP content of the sample was lower than the annotated one. These experiments indicate that **FD-F3** can detect the F^- content in toothpastes prepared with different F^- sources.

Fluoride, as an important anti-caries agent, can be absorbed by the dental plaque biofilm as a fluoride reservoir.[3,4] Visualizing

Table 1 Measurement of F^- from different toothpastes

Sample	F^- source	Proposed method (mg L^{-1})	FISE (mg L^{-1})	Calculations based on annotated content (mg L^{-1})
Sample A	NaF	13.68	10.43	14.22
Sample B	NaF	7.92	5.72	7.32
Sample C	SMFP	2.72	1.39	10.30

The data presented have been converted into the content of NaF or SMFP.

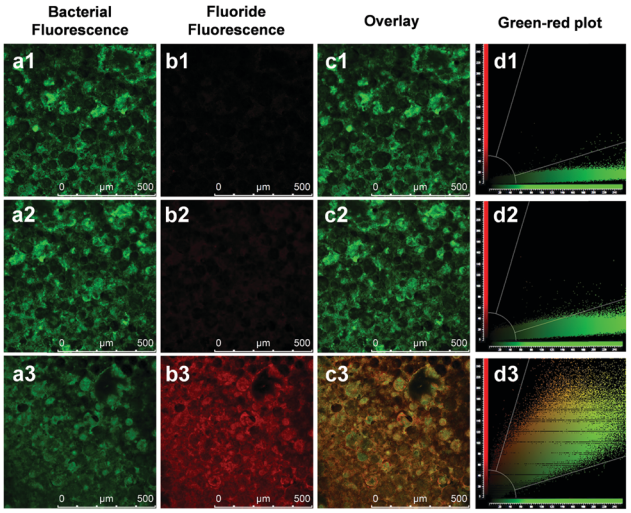

Fig. 2 CLSM images of F^- in human *in situ* plaque biofilms. (a1–d1), (a2–d2) and (a3–d3) show plaque biofilms treated with PBS, NFT and SFT for 2 min, respectively. (a1, a2, and a3) are green channels for SYTO® 9 probe staining (λ_{ex} = 488 nm, λ_{em} = 500–550 nm); (b1, b2, and b3) are near-infrared channels for **FD-F3** probe staining (λ_{ex} = 633 nm, λ_{em} = 670–720 nm); (c1, c2, and c3) are overlay images; (d1, d2, and d3) are green-red scattered plots of all non-black pixels of (c1, c2, and c3), respectively.

fluoride uptake into the dental plaque biofilm could be a useful tool for designing oral care compositions that can control plaque bacteria and enhance remineralization. Given the ability of **FD-F3** to visualize F^-, we attempted to visualize F^- in a dental plaque biofilm using a confocal laser scanning microscope (CLSM). Bacterial contents of the plaque biofilm were stained and visualized using the SYTO® 9 probe (5 μM, 0.2% DMSO (v/v) in PBS, Fig. 2(a1–a3)). Fluoride ions were also stained and visualized using **FD-F3** (5 μM 0.2% DMSO (v/v) in PBS, Fig. 2(b1–b3)). PBS solution (Fig. 2(a1–d1)) did not induce **FD-F3** fluorescence (red pixel% = 0.53 ± 0.07% as shown in Fig. 2d1), indicating that the chloride ions in PBS did not interfere with **FD-F3** fluorescence. Evaluation of marketed non-fluoride (Fig. 2(a2–d2)) and fluoride toothpastes (Fig. 2(a3–d3)) was conducted. The fluoride free toothpaste (NFT) induced a marginal NIR fluorescence (red pixel% = 7.26 ± 0.82% as shown in Fig. 2d2), possibly due to interference by the autofluorescence of abrasive particles. In contrast, a 2 min treatment with a sodium fluoride containing toothpaste (SFT), induced significant fluorescence of **FD-F3** (red pixel% = 91.33 ± 8.14% as shown in Fig. 2d3). These results suggest that the **FD-F3** probe could be used to distinguish between non-fluoride and fluoride toothpastes by visualizing fluoride uptake into naturally grown human plaque biofilms.

Since **FD-F3** could be used to visualize fluorides in naturally grown human plaque biofilms by releasing MB and MB is one of the most widely used agents for aPDT,[26,27] the F^- activated aPDT in the biofilm was then performed. The distribution of live and dead biofilm bacteria was simultaneously viewed by CLSM using the reagents SYTO 9 stain and propidium iodide in the LIVE/DEAD BacLight Bacterial Viability Kit. As shown in Fig. 3, when compared with control groups (Fig. 3a1 and a2), the proportion of dead bacteria showed no significant change

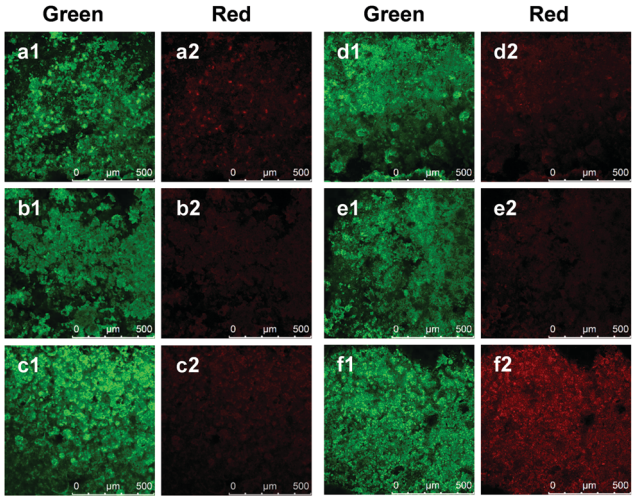

Fig. 3 CLSM images of human *in situ* plaque biofilms upon PDT treatment. (a1 and a2) Without any treatment as control; (b1 and b2) treated only with free **FD-F3** (50 μg mL^{-1}) for 30 min; (c1 and c2) with NaF (50 μg mL^{-1}) for 60 min; (d1 and d2) with **FD-F3** (50 μg mL^{-1}) for 30 min and then NaF (50 μg mL^{-1}) for 60 min; (e1 and e2) only with light (100 mW cm^{-2}) for 5 min; (f1 and f2) with **FD-F3** (50 μg mL^{-1}) for 30 min then NaF (50 μg mL^{-1}) for 60 min and then light (100 mW cm^{-2}) for 5 min. (a1, b1, c1, d1, e1, and f1) are green channels for SYTO® 9 probe staining (λ_{ex} = 488 nm, λ_{em} = 500–550 nm); (a2, b2, c2, d2, e2, and f2) are red channels for propidium iodide probe staining (λ_{ex} = 488 nm, λ_{em} = 600–650 nm).

when treated with free **FD-F3** (Fig. 3b1 and b2), NaF (Fig. 3c1 and c2), **FD-F3** + NaF (Fig. 3d1 and d2) or light (Fig. 3e1 and e2). However, the proportion of dead bacteria increased by 28% (Fig. S13, ESI†) when treated with **FD-F3** (50 μg mL^{-1}, 30 min), followed by NaF (50 μg mL^{-1}) for 60 min and then a laser (100 mW cm^{-2}) for 5 min (Fig. 3f1 and f2), indicating that **FD-F3** could be used as a F^- regulated prodrug for aPDT in naturally grown human plaque biofilms.

In summary, a series of novel fluorescent probes were designed and synthesized for sensing F^- and performing F^- activated aPDT, based on a new platform containing an MB derivative as the fluorophore. These probes are easily synthesized and show high selectivity toward F^- in an aqueous solution. Among them, the optimal one, **FD-F3**, exhibits a dramatic increase of NIR fluorescence and red absorption in the presence of F^-, which can be detected by the naked-eye. **FD-F3** can distinguish F^- from NaF and SMFP with a low detection limit and can be applied to determine the F^- content of toothpastes prepared using different F^- sources. Moreover, **FD-F3** can distinguish between non-fluoride and fluoride toothpastes by visualizing fluoride uptake into naturally grown human plaque biofilms. In addition, **FD-F3** could be used as a F^- regulated prodrug for antimicrobial photodynamic therapy. These fluoride activated probes thus provide a practical platform for monitoring F^- in biofilms, studying the physiological function of F^- in biological systems and designing a F^- regulated prodrug for antimicrobial photodynamic therapy.

The authors acknowledge the financial support from NNSFC (21877013 and 21671043) and the National Key R&D Program of China (2017YFA0205100).

Conflicts of interest

There are no conflicts to declare.

References

1 A. Ammari, A. Bloch-Zupan and P. Ashley, *Caries Res.*, 2003, **37**, 85–92.
2 W. M. Edmunds and P. L. Smedley, in *Essentials of Medical Geology: Revised Edition*, ed. O. Selinus, Springer Netherlands, Dordrecht, 2013, pp. 311–336, DOI: 10.1007/978-94-007-4375-5_13.
3 J. A. Cury and L. M. A. Tenuta, *Adv. Dent. Res.*, 2008, **20**, 13–16.
4 H.-C. Flemming, T. R. Neu and D. J. Wozniak, *J. Bacteriol.*, 2007, **189**, 7945–7947.
5 D. L. Ozsvath, *Rev. Environ. Sci. Bio/Technol.*, 2009, **8**, 59–79.
6 Z. Wang, G. Ma and X. Y. Liu, *J. Phys. Chem. B*, 2009, **113**, 16393–16399.
7 D. Browne, H. Whelton and D. O'Mullane, *J. Dent.*, 2005, **33**, 177–186.
8 X. Xiong, J. Liu, W. He, T. Xia, P. He, X. Chen, K. Yang and A. Wang, *Environ. Res.*, 2007, **103**, 112–116.
9 L. Gai, J. Mack, H. Lu, T. Nyokong, Z. Li, N. Kobayashi and Z. Shen, *Coord. Chem. Rev.*, 2015, **285**, 24–51.
10 Y. Zhou, J. F. Zhang and J. Yoon, *Chem. Rev.*, 2014, **114**, 5511–5571.
11 J. Xu, S. Sun, Q. Li, Y. Yue, Y. Li and S. Shao, *Anal. Chim. Acta*, 2014, **849**, 36–42.
12 S. Y. Kim, J. Park, M. Koh, S. B. Park and J.-I. Hong, *Chem. Commun.*, 2009, 4735–4737.
13 J.-T. Yeh, P. Venkatesan and S.-P. Wu, *New J. Chem.*, 2014, **38**, 6198–6204.
14 B. Zhu, F. Yuan, R. Li, Y. Li, Q. Wei, Z. Ma, B. Du and X. Zhang, *Chem. Commun.*, 2011, **47**, 7098–7100.
15 C.-Q. Zhu, J.-L. Chen, H. Zheng, Y.-Q. Wu and J.-G. Xu, *Anal. Chim. Acta*, 2005, **539**, 311–316.
16 Z. Wu and X. Tang, *Anal. Chem.*, 2015, **87**, 8613–8617.
17 B. Ke, W. Chen, N. Ni, Y. Cheng, C. Dai, H. Dinh and B. Wang, *Chem. Commun.*, 2013, **49**, 2494–2496.
18 L. Li, Y. Ji and X. Tang, *Anal. Chem.*, 2014, **86**, 10006–10009.
19 C. Padié and K. Zeitler, *New J. Chem.*, 2011, **35**, 994–997.
20 N. Busschaert, C. Caltagirone, W. Van Rossom and P. A. Gale, *Chem. Rev.*, 2015, **115**, 8038–8155.
21 G. Feng, L. Geng, T. Wang, J. Li, X. Yu, Y. Wang, Y. Li and D. Xie, *J. Lumin.*, 2015, **167**, 65–70.
22 L. Geng, G. Feng, S. Wang, X. Yu, Z. Xu, X. Zhen and T. Wang, *J. Fluorine Chem.*, 2015, **170**, 24–28.
23 R. Li, S. Wang, Q. Li, H. Lan, S. Xiao, Y. Li, R. Tan and T. Yi, *Dyes Pigm.*, 2017, **137**, 111–116.
24 X. Yu, D. Xie, Y. Li, L. Geng, J. Ren, T. Wang and X. Pang, *Sens. Actuators, B*, 2017, **251**, 828–835.
25 T. H. Kim and T. M. Swager, *Angew. Chem., Int. Ed.*, 2003, **42**, 4803–4806.
26 F. Cieplik, D. Deng, W. Crielaard, W. Buchalla, E. Hellwig, A. Al-Ahmad and T. Maisch, *Crit. Rev. Microbiol.*, 2018, **44**, 571–589.
27 S. Rajesh, E. Koshi, K. Philip and A. Mohan, *J. Indian Soc. Periodontol.*, 2011, **15**, 323–327.
28 F. Xue, P. Wei, X. Ge, Y. Zhong, C. Cao, D. Yu and T. Yi, *Dyes Pigm.*, 2018, **156**, 285–290.
29 P. Wei, W. Yuan, F. Xue, W. Zhou, R. Li, D. Zhang and T. Yi, *Chem. Sci.*, 2018, **9**, 495–501.
30 G. Wei, J. Yin, X. Ma, S. Yu, D. Wei and Y. Du, *Anal. Chim. Acta*, 2011, **703**, 219–225.
31 F. Zheng, F. Zeng, C. Yu, X. Hou and S. Wu, *Chem. – Eur. J.*, 2013, **19**, 936–942.
32 S. T. SebaSTian and S. SiDDanna, *J. Clin. Diagn. Res.*, 2015, **9**, ZC09.

